

Palladium-Catalyzed Carbene Migratory Insertion Using Conjugated Ene–Yne–Ketones as Carbene Precursors

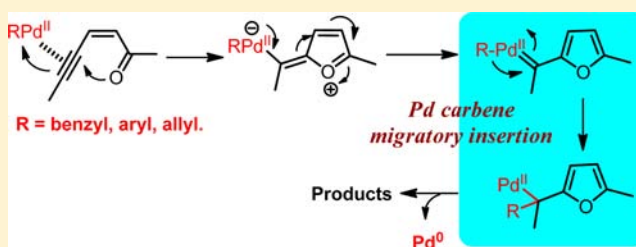
Ying Xia,^{†,§} Shuanglin Qu,^{‡,§} Qing Xiao,^{†,§} Zhi-Xiang Wang,^{*,‡} Peiyuan Qu,[†] Li Chen,[†] Zhen Liu,[†] Leiming Tian,[†] Zhongxing Huang,[†] Yan Zhang,[†] and Jianbo Wang^{*,†}

[†]Beijing National Laboratory of Molecular Sciences (BNLMS), Key Laboratory of Bioorganic Chemistry and Molecular Engineering of the Ministry of Education, College of Chemistry, Peking University, Beijing 100871, China

[‡]School of Chemistry and Chemical Engineering, University of Chinese Academy of Sciences, Beijing 100049, China

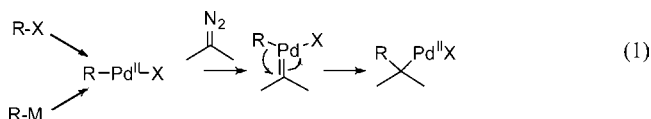
S Supporting Information

ABSTRACT: Palladium-catalyzed cross-coupling reactions between benzyl, aryl, or allyl bromides and conjugated ene–yne–ketones lead to the formation of 2-alkenyl-substituted furans. This novel coupling reaction involves oxidative addition, alkyne activation–cyclization, palladium carbene migratory insertion, β -hydride elimination, and catalyst regeneration. Palladium (2-furyl)carbene is proposed as the key intermediate, which is supported by DFT calculations. The palladium carbene character of the key intermediate is validated by three aspects, including bond lengths, Wiberg bond order indices, and molecular orbitals, by comparison to those reported for stable palladium carbene species. Computational studies also revealed that the rate-limiting step is ene–yne–ketone cyclization, which leads to the formation of the palladium (2-furyl)carbene, while the subsequent carbene migratory insertion is a facile process with a low energy barrier (<5 kcal/mol).



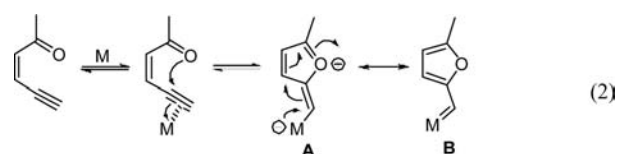
INTRODUCTION

Transition-metal-catalyzed cross-coupling reactions involving diazo compounds or *N*-tosylhydrazones as coupling partners have emerged as a practical synthetic method for C–C and C=C bond formation.^{1,2} In particular, with palladium catalysts, diazo compounds or *N*-tosylhydrazones can be coupled with benzyl halides,^{3a,b} aryl halides,^{3c,d} allyl halides,^{3e} and other electrophiles.^{3f–i} Under oxidative conditions, they can also be coupled with nucleophiles such as arylboronic acids^{4a–c} and terminal alkynes.^{4d} In these transformations, formation of the palladium carbene and the subsequent migratory insertion is proposed to play the key role in amalgamating the classical cross-coupling and carbene chemistry (eq 1).^{5,6}



Diazo compounds, either used directly or generated in situ from *N*-tosylhydrazones, have served as the common precursors in various catalytic carbene transfer reactions.⁷ This has also been the case for the newly developed cross-coupling reactions involving palladium carbenes, as shown in eq 1. The obvious drawback of diazo compounds is their explosive and toxic nature. It is thus highly desirable to search for alternative precursors for metal carbenes. In this context, the activation of alkynes with transition metals to generate carbenoid species, which can serve as safe and effective alternatives to diazo decomposition, has

received considerable attention in past years.⁸ For example, the transition-metal-catalyzed cycloisomerization of ene–yne–ketones has been explored by Uemura and Ohe⁹ and more recently by Vicent and López¹⁰ and others.¹¹ In those transformations, the alkyne moiety is activated by a transition metal, which is then attacked by the carbonyl oxygen through 5-exo-dig cyclization to form zwitterionic intermediate **A** or its resonance structure, metal (2-furyl)carbene complex **B** (eq 2).



can subsequently participate in various transformations, such as cyclopropanation, ylide formation, X–H insertion, and other related reactions.^{9–12} For example, Ohe, Uemura, and co-workers reported the polymerization of ene–yne–ketones through Rh(II) (2-furyl)carbene [**B** with M = Rh(II)].^{9e} Vicente, López, and co-workers demonstrated that Zn(II) (2-furyl)carbenes [**B** with M = Zn(II)] obtained from ene–yne–ketones undergo cyclopropanation and X–H (X = O, Si) insertions.¹⁰ More recently, Jiang and co-workers reported the oxidation of Cu(I) (2-furyl)carbenes [**B** with M = Cu(I)] from ene–yne–ketones.^{11b} These studies demonstrate that metal (2-furyl)carbene

Received: June 12, 2013

Published: August 15, 2013

formation from ene-yne-ketones is general and that these carbenes may undergo various transformations.


In connection with our interest in cross-coupling reactions involving palladium carbenes, we conceived the possibility of developing precursors other than diazo compounds for palladium carbene generation. In this way, analogous palladium-catalyzed cross-coupling reactions between electrophiles and various metal carbene precursors (eq 1) should be realized, thus significantly expanding the scope of such coupling reactions. To verify this conjecture, we chose the ene-yne-ketone system to generate palladium (2-furyl)carbenes [B, M = Pd-R]. We expected similar palladium carbene migratory insertion to occur from the palladium (2-furyl)carbenes generated in this way. Herein we report the palladium-catalyzed cross-coupling reaction between ene-yne-ketones and benzyl, aryl, or allyl bromides. The reaction is efficient and tolerates various functional groups, affording 2-alkenyl-substituted furans in moderate to good yields. Density functional theory (DFT) calculations revealed the details of the reaction mechanism, which includes oxidative addition, alkyne activation-cyclization, palladium carbene migratory insertion, β -hydride elimination, and catalyst regeneration. The DFT calculations support the involvement of palladium (2-furyl)carbene as the reactive intermediate and also indicate that the migratory insertion is a facile process with a low energy barrier (<5 kcal/mol).

RESULTS

The ene-yne-ketone substrates **1a–o** were easily prepared via Knoevenagel condensation of conjugated yne-aldehydes with 1,3-dicarbonyl compounds.¹³ With these substrates in hand, we first studied their coupling reactions with benzyl bromides. At the outset of this investigation, ene-yne-ketone **1a** and 4-methylbenzyl bromide (**2a**) were employed as the substrates (Table 1). We were delighted to find that in the presence of 2.5 mol % Pd₂(dba)₃, 20 mol % P(2-furyl)₃, and 3 equiv of Cs₂CO₃, the expected 2-alkenyl-substituted furan **3a** was obtained in 33% yield (entry 1). By screening the palladium catalyst, we found that simple Pd(PPh₃)₄ could afford a higher yield (entry 2). A series of bases were then tested with Pd(PPh₃)₄ as the catalyst (entries 3–7).¹⁴ We found that the organic base ^tPr₂NEt gave the best result, improving the yield to 62% (entry 5). Through further inspection of the solvent, we found that *N,N*-dimethylformamide (DMF) was more suitable for this transformation (entries 8–13). Interestingly, the bulky and electron-rich XPhos ligand made this transformation sluggish, and only a moderate yield was obtained when the reaction time was extended to 12 h (entry 14). Thus, the optimal reaction conditions were found to be Pd(PPh₃)₄ as the catalyst, ^tPr₂NEt as the base, and DMF as the solvent (entry 13). It is noteworthy that only one stereoisomer was obtained in this reaction. The configuration of the formed double bond of **3a** was confirmed to be *Z* through nuclear Overhauser effect spectroscopy (NOESY) experiments. The excellent *Z* stereoselectivity can be rationalized by the transition state of the β -hydride elimination of the palladium intermediate, in which a strong interaction between the arene and the *tert*-butyl group is avoided.

The scope of this transformation was first explored by using various ene-yne-ketones **1a–j** and **2a** (Scheme 1). The influence of the R¹ group, which is adjacent to the alkyne moiety, was explored first (**3a–d**). When the *tert*-butyl group was changed to the less hindered trimethylsilyl (TMS) group, the product **3b** was obtained in slightly improved yield, albeit with decreased selectivity. The bulky triisopropylsilyl (TIPS) group made this

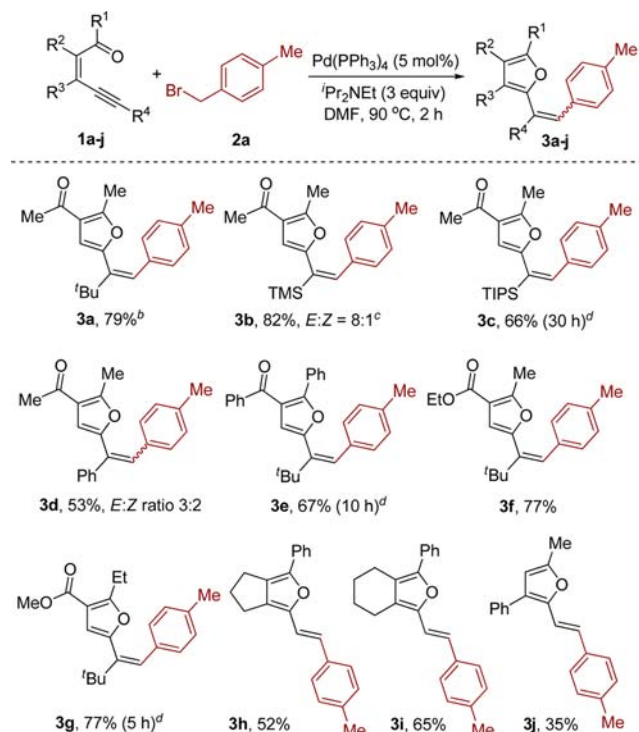
Table 1. Optimization Experiments for the Reaction of Ene-Yne-Ketone **1a and 4-Methylbenzyl Bromide (**2a**)^a**



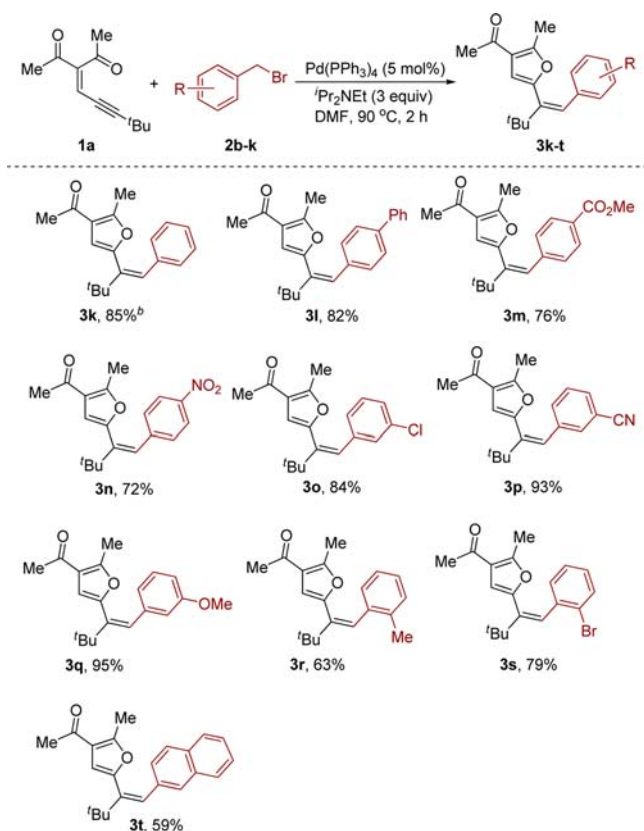
entry	Pd (mol %)/ligand (mol %)	base	solvent	yield (%) ^b
1	Pd ₂ (dba) ₃ (2.5)/P(2-furyl) ₃ (20)	Cs ₂ CO ₃	MeCN	33
2	Pd(PPh ₃) ₄ (5)	Cs ₂ CO ₃	MeCN	40
3	Pd(PPh ₃) ₄ (5)	K ₂ CO ₃	MeCN	43
4	Pd(PPh ₃) ₄ (5)	LiO ^t Bu	MeCN	trace
5	Pd(PPh ₃) ₄ (5)	^t Pr ₂ NEt	MeCN	62
6	Pd(PPh ₃) ₄ (5)	DBU	MeCN	trace
7	Pd(PPh ₃) ₄ (5)	^t Pr ₂ NH	MeCN	51
8	Pd(PPh ₃) ₄ (5)	^t Pr ₂ NEt	toluene	22
9	Pd(PPh ₃) ₄ (5)	^t Pr ₂ NEt	dioxane	25
10	Pd(PPh ₃) ₄ (5)	^t Pr ₂ NEt	DCE	34
11	Pd(PPh ₃) ₄ (5)	^t Pr ₂ NEt	THF	28
12	Pd(PPh ₃) ₄ (5)	–	1:1 ^t Pr ₂ NEt/MeCN	46
13	Pd(PPh ₃) ₄ (5)	^t Pr ₂ NEt	DMF	79
14 ^c	Pd ₂ (dba) ₃ (2.5)/XPhos (15)	^t Pr ₂ NEt	DMF	49

^aThe reaction was carried out with **1a** (0.24 mmol) and **2a** (0.20 mmol) in 2.0 mL of solvent at 90 °C for 2 h. ^bYields of products isolated by column chromatography. ^cThe reaction time was 12 h.

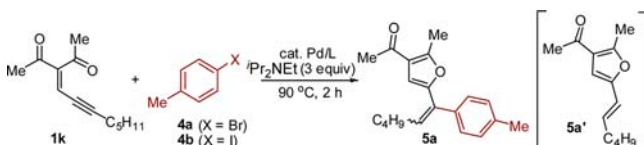
Scheme 1. Scope of Ene-Yne-Ketones in the Pd-Catalyzed Coupling Reaction^a



^aUnless otherwise noted, the reactions were carried out with **1a–j** (0.24 mmol), **2a** (0.2 mmol), Pd(PPh₃)₄ (5 mol %), and ^tPr₂NEt (0.6 mmol) in DMF (2.0 mL) at 90 °C for 2 h. ^bYields of products isolated by column chromatography are shown. ^c*E*/*Z* ratios were determined by GC–MS. ^dThe number in parentheses is the reaction time.

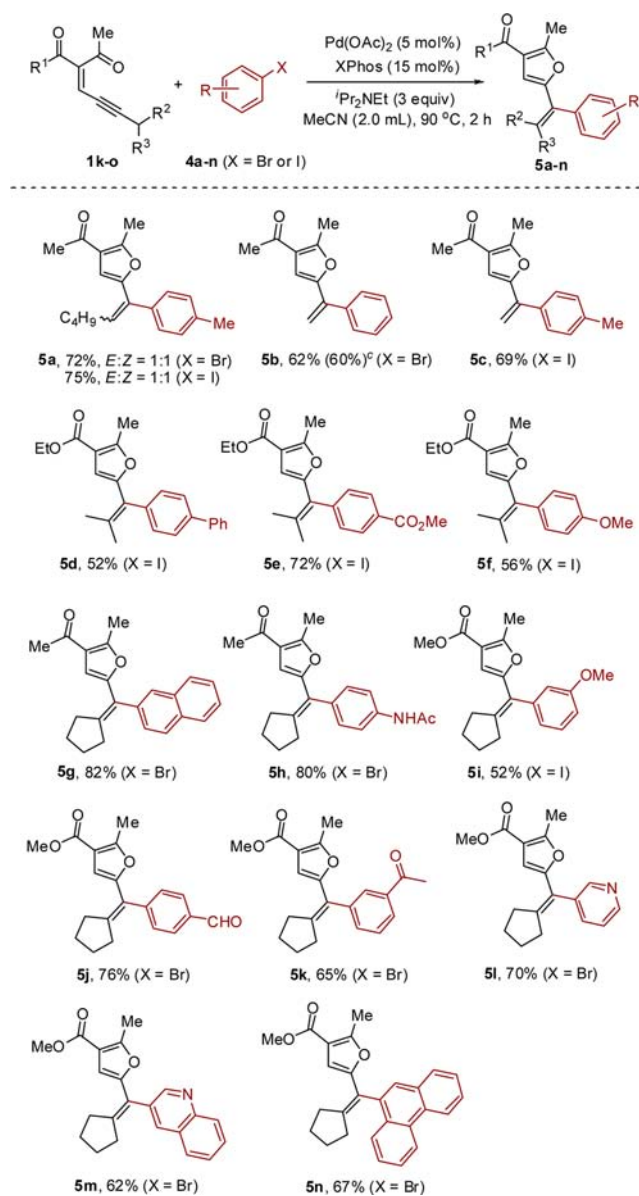
Scheme 2. Scope of Benzyl Bromides in the Pd-Catalyzed Coupling Reaction^a

^aReactions were carried out with **1a** (0.24 mmol) and **2** (0.2 mmol), Pd(PPh₃)₄ (5 mol %), and ^tPr₂NEt (0.6 mmol) in DMF (2.0 mL) at 90 °C for 2 h. ^bYields of products isolated by column chromatography are shown.

Table 2. Optimization Experiments for the Reaction of Ene-Yne-Ketone **1a** and 4-Bromotoluene (**4a**) or 4-Iodotoluene (**4b**)^a

entry	Pd (mol %)/ligand (mol %)	solvent	yield (%) ^b
1	Pd(PPh ₃) ₄ (5)	DMF	25
2	Pd ₂ (dba) ₃ (2.5)/XPhos(15)	DMF	40
3	Pd ₂ (dba) ₃ (2.5)/XPhos(15)	dioxane	19
4	Pd ₂ (dba) ₃ (2.5)/XPhos(15)	MeCN	65
5	Pd ₂ (dba) ₃ (2.5)/XPhos(15)	toluene	29
6	Pd ₂ (dba) ₃ (2.5)/XPhos(15)	DCE	31
7 ^c	Pd ₂ (dba) ₃ (2.5)/XPhos(15)	MeCN	trace
8 ^d	Pd ₂ (dba) ₃ (2.5)/XPhos(15)	MeCN	42
9	Pd ₂ (dba) ₃ (2.5)/PCy ₃ (15)	MeCN	23
10	Pd ₂ (dba) ₃ (2.5)/2-PhC ₆ H ₄ PCy ₂ (15)	MeCN	34
11	Pd(OAc) ₂ (5)/XPhos(15)	MeCN	68
12 ^e	Pd(OAc) ₂ (5)/XPhos(15)	MeCN	72
13 ^{e,f}	Pd(OAc) ₂ (5)/XPhos(15)	MeCN	75

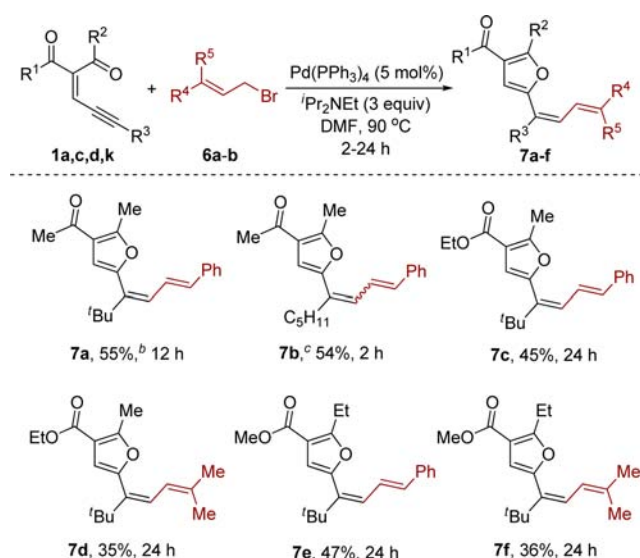
^aThe reaction was carried out with **4a** (0.20 mmol), **1k** (0.24 mmol) and ^tPr₂NEt (0.6 mmol) in 2.0 mL of solvent, unless otherwise noted. ^bIsolated yields. ^cCS₂CO₃ was used as the base instead of ^tPr₂NEt. ^d^tPr₂NH was used as the base instead of ^tPr₂NEt. ^e0.26 mmol of **1k** was used. ^fThe reaction was carried out using **4b**.

Scheme 3. Pd-Catalyzed Couplings of Ene-Yne-Ketones and Aryl Halides^{a,b}

^aReactions were carried out with **1** (0.26 mmol), **4** (0.2 mmol), Pd(OAc)₂ (5 mol %), XPhos (15 mol %), and ^tPr₂NEt (0.6 mmol) in MeCN (2.0 mL) at 90 °C for 2 h. ^bIsolated yields are shown. ^cThe yield in parentheses was obtained by using Pd₂(dba)₃ (2.5 mol %) in place of Pd(OAc)₂ (5 mol %).

transformation sluggish. The reaction was completed in 30 h, affording **3c** in 66% yield. Compared with **1b**, the slow reaction of **1c** may result from the difficulty of activation of the triple bond by the palladium complex due to the greater steric hindrance of the TIPS group compared with the TMS group. However, the bulky TIPS group afforded complete control of the stereo-selectivity. For R⁴ = phenyl, the corresponding product **3d** was also obtained in moderate yield, but the selectivity was poor because of the similar steric bulk of the phenyl and furyl moieties.

The influence of the nucleophilic carbonyl oxygen was also explored (**3f**, **3g**). In the preparation of ene-yne-ketones **1f** and **1g** via Knoevenagel condensation of the conjugated yne-aldehyde with unsymmetrical 1,3-dicarbonyl compounds, a

Scheme 4. Pd-Catalyzed Coupling Reaction of Ene–Yne–Ketones and Allyl Bromides^a

^aReactions were carried out with **1** (0.24 mmol), **6** (0.2 mmol), Pd(PPh₃)₄ (5 mol %), and ⁱPr₂NEt (0.6 mmol) in DMF (2.0 mL) at 90 °C for indicated times. ^bIsolated yields are shown. ^cAlthough a single product was isolated, the configuration of the newly formed double bond could not be confirmed by NMR analysis.

Scheme 5. Proposed Catalytic Cycle

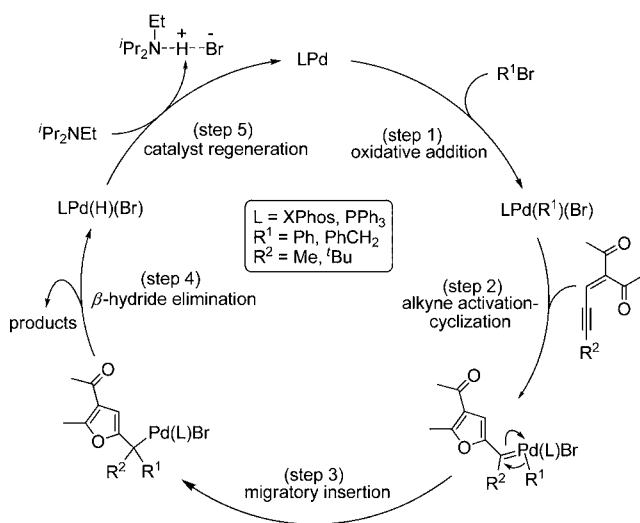


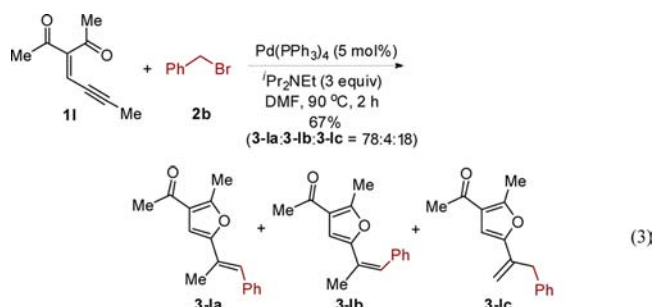
Table 3. Highest Free Energy Barriers (in kcal/mol) for the Steps Involved in the Catalytic Cycle

reaction	step 1	step 2	step 3	step 4	step 5
eq 4	13.1	22.4	4.6	15.7	7.2
eq 5	3.0	26.1	3.6	15.0	17.4

mixture of *E*- and *Z*-isomeric products was obtained in about a 1:1 ratio, and they were difficult to separate. However, to our delight, the mixture of (*E*)- and (*Z*)-ene-yne-ketones **1f** and **1j** smoothly afforded the corresponding 2-alkenyl-substituted furans **3f** and **3j**, respectively, as single products. This indicates that isomerization of the double bonds in **1f** and **1j** occurs easily during the course of the reaction.¹⁵ Moreover, it is noted that only the ketone carbonyl oxygen attacks the activated alkyne

moiety, while the ester carbonyl oxygen cannot undergo the similar process because of its lower nucleophilicity.^{11b,c} Besides, in view of the reaction times, the reaction of **1g** was slower than those of **1a** and **1f**, and benzoyl-type ene-yne-ketone **1e** showed a much slower reaction. These results indicate that the reactivity of the carbonyl oxygens in this transformation are ordered as follows: acetyl > propionyl > benzoyl ≫ ester.^{11b,c} Finally, we found that other types of ene-yne-ketones could also undergo similar reactions, although the yields were diminished (**3h–j**). The low yields in these cases are attributed to the instability of both the substrates and the products under the reaction conditions.

For R⁴ = methyl (**11**), three isomers (**3-la**, **3-lb**, and **3-lc**) can be obtained depending on the selectivity of the β-hydride elimination (eq 3). The ratio of the three isomers was 78:4:18, indicating that the benzyl hydride elimination afforded the major product with excellent *E* stereoselectivity.¹³



We then investigated the scope of benzyl bromides in this palladium-catalyzed transformation (Scheme 2). The coupling of ene-yne-ketone **1a** with benzyl bromide (**2b**) produced the target product **3k** in good yield. This reaction was used as the model reaction for the computational studies. It was found that the coupling is not significantly affected by the substituents on the aromatic ring of the benzyl bromide. Both electron-rich (**3q**, **3r**, **3t**) and electron-deficient (**3m–p**, **3s**) benzyl bromides afforded the corresponding furan products in good yields. Remarkably, ester, nitro, chloro, cyano, and alkoxy groups all were well-tolerated under the standard reaction conditions. Interestingly, the aryl bromides were less active than the corresponding benzyl bromides under the optimized reaction conditions, and the bromo substituent did not interfere the reaction in the case of **3s**.

Next, we investigated a similar reaction between ene-yne-ketones and aryl halides **4**. In these reactions, in order to meet the requirement of β-hydride elimination of the palladium species in the final step of the catalytic cycle, the substituent adjacent to the terminal alkyne moiety of the ene-yne-ketone should have hydrogen. Consequently, we employed ene-yne-ketone **1k**, in which *n*-C₅H₁₁ is the substituent of the alkyne moiety, along with 4-bromotoluene (**4a**) to optimize the reaction conditions (Table 2). When the standard reaction conditions for the corresponding coupling reaction of benzyl bromides and ene-yne-ketones were employed, only a 25% yield of the expected coupling product could be obtained (entry 1). The yield improved to 40% when the bulky and electron-rich XPhos ligand was used (entry 2). The solvent and base were then screened. It was found that MeCN showed superior results compared with DMF. When ⁱPr₂NEt was used as the base, the best results were obtained in this coupling reaction (entries 3–8). At this point, the yield was optimized to 65% (entry 4). Changing XPhos to the less bulky ligand PCy₃ or 2-PhC₆H₄PCy₂ resulted in poor yields (entries 9 and 10), indicating that the isopropyl groups on XPhos

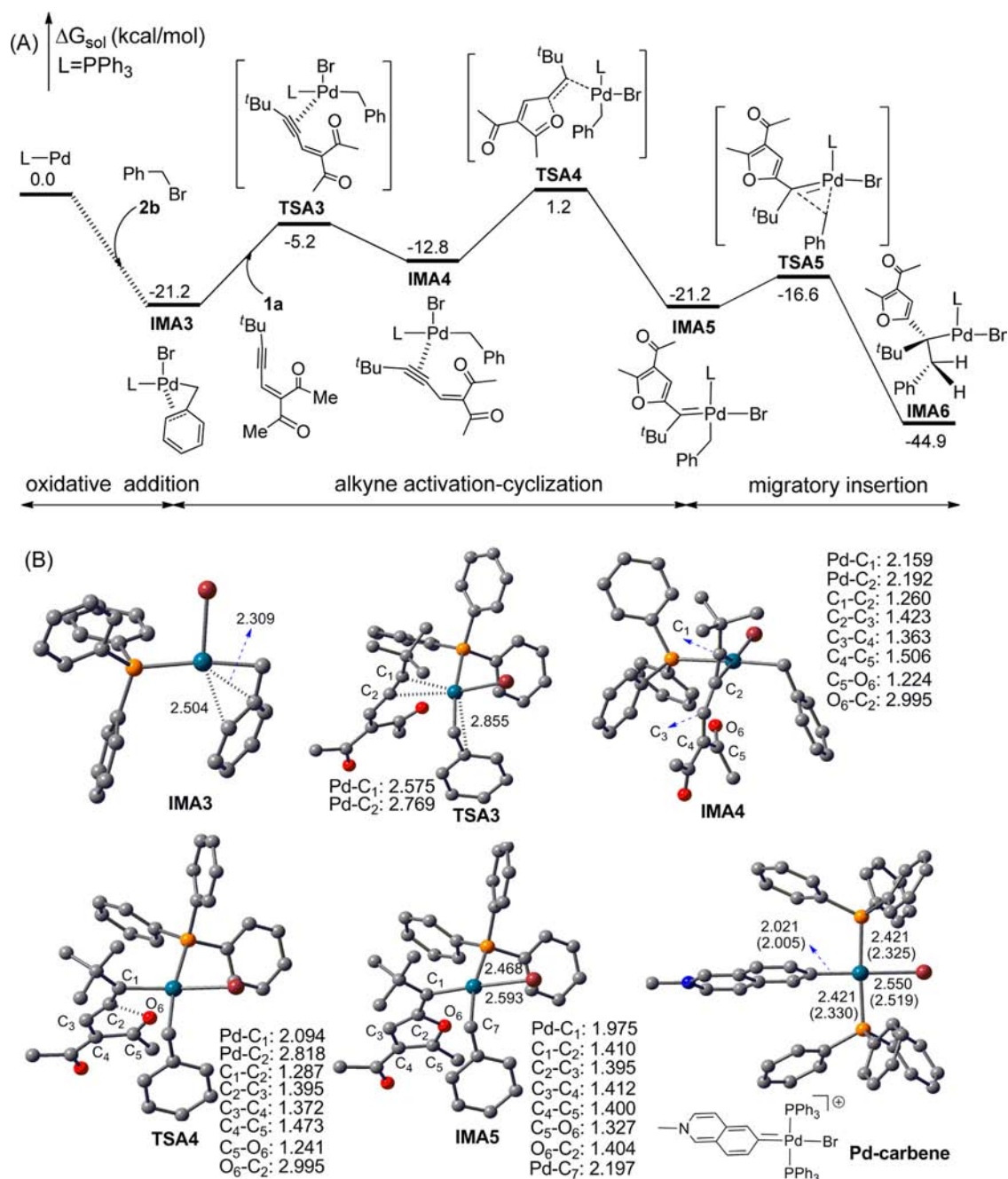


Figure 1. (A) Free energy profile for steps 2 and 3 in the reaction shown in eq 4. (B) Optimized structures of key stationary points together with key bond lengths (in Å). The values in parentheses in **Pd-carbene** are bond lengths reported in its X-ray structure.^{21e} Trivial H atoms have been omitted.

are essential. With the combination of XPhos and $\text{Pd}(\text{OAc})_2$ as the catalyst, the yield of the reaction could be improved slightly (entry 11). During optimization of this reaction, we found that the major side product was **5a'**, which might be generated from β -hydride elimination/reductive elimination sequences or a direct 1,2-hydride shift of the palladium carbene intermediate.^{8g,11c,16} By slightly increasing the ratio of the ene-yne-ketone **1k**, we finally obtained 2-alkenyl-substituted furan **5a** in 72% yield (entry 12). In this reaction, 4-iodotoluene (**4b**) also gave the target product **5a** in a similar yield (entry 13). In all cases, the product was obtained as a 1:1 mixture of the *E* and *Z* isomers according to ¹H NMR analysis of the isolated product. Again, this is attributed to the similar size of the phenyl and furyl groups, which show little difference in the β -hydride elimination of the palladium intermediate.

Next, we explored the scope of this reaction using the series of aryl bromides or iodides **4a-n** and ene-yne-ketones **1k-o** under the optimized reaction conditions (Scheme 3). The coupling of ene-yne-ketone **1l** ($R^1 = \text{Me}$, $R^2 = R^3 = \text{H}$) with bromobenzene (**4c**) afforded 1,1-disubstituted alkene **5b** in 62% yield. When $\text{Pd}_2(\text{dba})_3$ was used in place of $\text{Pd}(\text{OAc})_2$, a similar yield was obtained. This reaction was used as the model reaction for the computational studies. The reaction of 4-iodotoluene with **1l** also gave the corresponding product in good yield (**5c**). When R^2 and R^3 were not hydrogen, tetrasubstituted olefins were obtained in moderate to good yields (**5d-n**). It is noteworthy that both electron-rich (**5f-i**, **5n**) and electron-deficient (**5e**, **5j-m**) aryl halides underwent this transformation smoothly. In addition, bromonaphthalene and bromophenanthrene

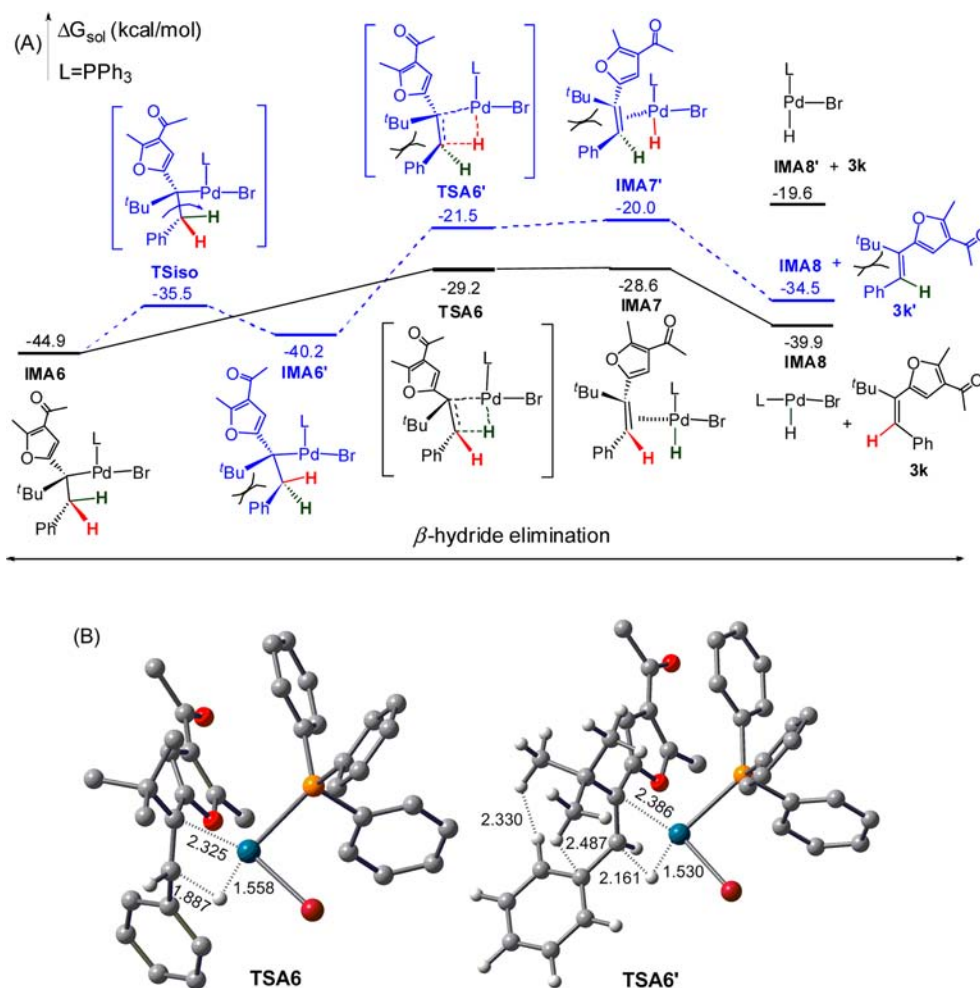


Figure 2. (A) Pathways for the β -hydride elimination step in the reaction shown in eq 4 along with relative free energies. (B) Key optimized structures with selected bond lengths (in Å). Trivial hydrogen atoms have been omitted for clarity.

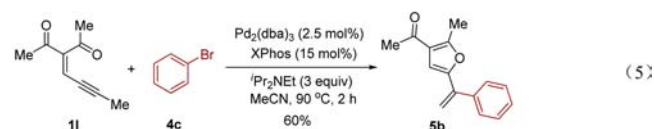
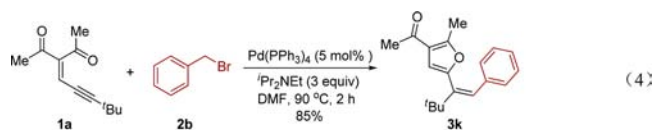
were also suitable substrates in this reaction (**5g**, **5n**). Finally, we found that the reaction conditions could also tolerate heteroaryl bromides, giving olefins bearing two heteroaryl substituents in good yields (**5l**, **5m**).

Finally, we investigated the reaction between ene-yne-ketones and allyl bromides (Scheme 4). Considering the similarity between allyl bromide and benzyl bromide, we applied the reaction conditions used for the reaction with benzyl bromide to the similar reaction with allyl bromide. However, we found that the reaction was sluggish for the latter case. For the coupling of ene-yne-ketone **1a** with allyl bromide **6a**, 2 h was not enough for complete conversion; the reaction time was extended to 12 h, but compound **7a** was obtained in only moderate yield. Further optimization failed to improve the yield of the reaction, probably because of the bulky *tert*-butyl group, which hinders the cyclization process in the transformation. When the substrate bearing the less bulky pentyl substituent was used, the reaction was significantly improved and could be finished in 2 h, albeit with moderate yield (**7b**). Other ene-yne-ketones and allyl bromides could also be applied to the reaction, affording the corresponding furyl-containing 1,3-butadiene derivatives **7c–f** in acceptable yields.

MECHANISTIC CONSIDERATIONS

To gain insight into the reaction mechanism, in particular to corroborate the involvement of palladium carbene intermediates in these transformations, we performed a DFT mechanistic study

using Gaussian 09.^{17,18} Both phenyl and benzyl bromides can couple with ene-yne-ketones, so we chose two experimental reactions (i.e., eqs 4 and 5) as representatives for mechanistic investigation. It has been reported that the catalytically active species in palladium-catalyzed C–C couplings are often monophosphine palladium complexes (i.e., LPd)^{19,20} when bulky phosphine ligands such as PPh₃,^{19b} P^{*t*}Bu₃,^{19d} and XPhos²⁰ are applied. We thus employed PPh₃Pd and XPhosPd as the active catalysts in the computations, where the actual ligands (PPh₃ and XPhos) were used without any simplification. Nevertheless, we also used the bisphosphine palladium complex (PPh₃)₂Pd as an active catalyst to validate the reasonability of using PPh₃Pd, and we found (PPh₃)₂Pd to be energetically less favorable than PPh₃Pd (vide infra).



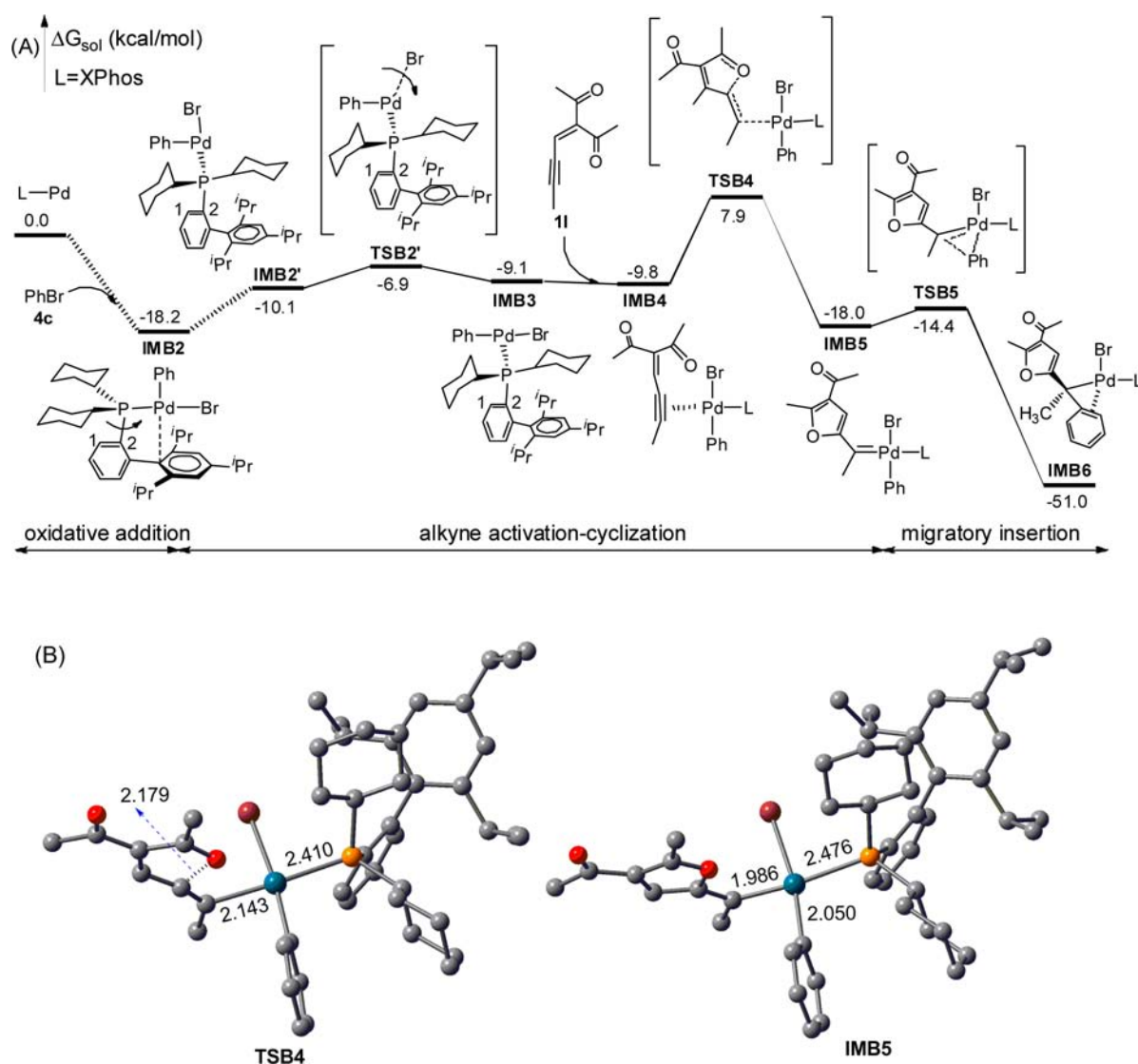


Figure 3. (A) Free energy profile for steps 2 and 3 in the reaction shown in eq 5. (B) Optimized structures of key stationary points together with key bond lengths (in Å). Trivial H atoms have been omitted.

Scheme 5 illustrates our proposed catalytic cycle, which can be characterized by five steps, namely, oxidative addition (step 1), alkyne activation–cyclization (step 2), palladium carbene migratory insertion (step 3), β -hydride elimination (step 4), and catalyst regeneration (step 5). Among the five steps, steps 1, 4, and 5 are similar to those in classical Heck reactions.^{19f}

Table 3 presents the highest free energy barrier (the free energy difference between the highest transition state and the lowest intermediate in each step) of each step, and the data show that step 2 is the rate-determining step for both reactions. The detailed energetic and geometric results for steps 1 and 5 are given in the Supporting Information, and hereafter we focus on the key steps 2–4: steps 2 and 3 involve palladium carbene intermediates, and step 4 determines the stereoselectivity.

The free energy profile for steps 2 and 3 in the reaction shown in eq 4 is given in Figure 1, together with the optimized structures of the key stationary points. The oxidative addition affords π complex **IMA3**, as reflected by the two short Pd–C bond distances (2.504 and 2.309 Å). The subsequent coordination of **1a** to **IMA3** breaks the π coordination by overcoming a barrier of 16.0 kcal/mol (**TSA3**) to form alkyne-coordinated π complex

IMA4, which is followed by cyclization via **TSA4** to give **IMAS**. The palladium intermediate **IMAS** features metal carbene character, as validated by comparison with well-characterized palladium carbenes whose crystal structures have been reported previously.²¹ As an example, we specifically compared **IMAS** with the cationic Pd-carbene in Figure 1B^{21e} because they have similar coordination environments. The formal Pd=C double bond in **IMAS** (1.975 Å) is shorter than those in the X-ray (2.005 Å) and computed (2.021 Å) structures of Pd-carbene, and the Wiberg bond index²² of the bond in the former (0.699) is larger than that in the latter (0.587). Furthermore, as compared in Figure S4 in the Supporting Information, they have very similar σ and π orbitals involved in the formal Pd=C bonds. However, the palladium carbene species (**IMAS**) is not stable; the benzyl group can easily migrate to the C₁ atom by striding a low barrier of 4.6 kcal/mol (**TSA5**), leading to intermediate **IMA6**, which is much more stable than **IMAS** (by 23.7 kcal/mol). Overall, the process from **IMA3** + **1a** to **IMA6** overcomes a barrier of 22.4 kcal/mol and is exergonic by 23.7 kcal/mol, indicating that the process can proceed feasibly.

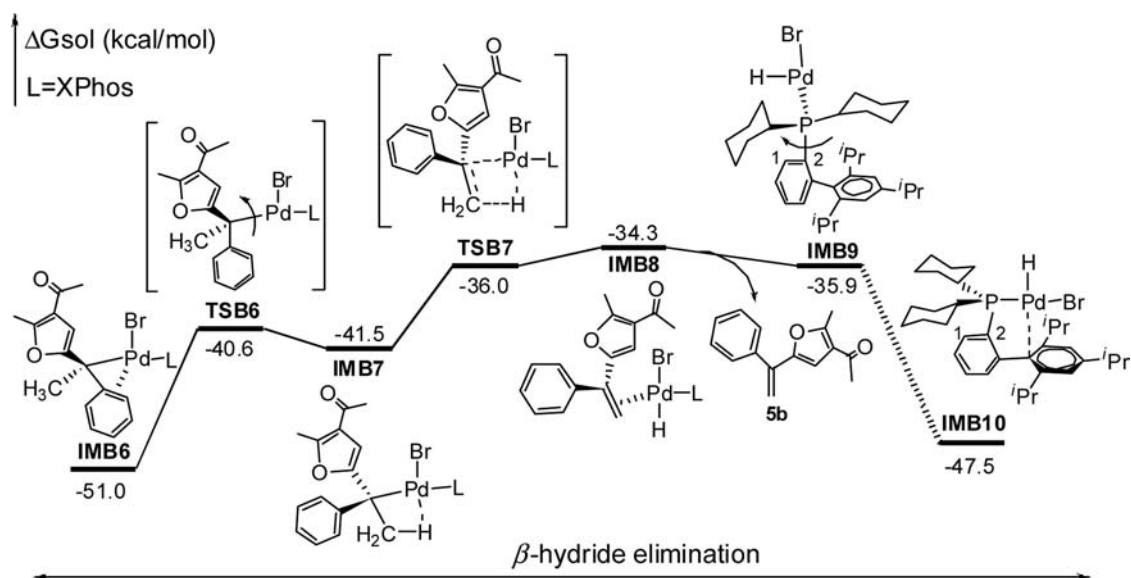


Figure 4. Free energy profile for the β -hydride elimination step in the reaction shown in eq 5. The barrier for the rotation around the P–C₂ bond in going from **IMB9** to **IMB10** was estimated to be about 12.0 kcal/mol through PES scanning (Figure S9 in the Supporting Information).

Subsequent to the migratory insertion to form **IMA6**, the β -hydride elimination takes place. Along the black pathway in Figure 2, the β -hydride elimination climbs a barrier of 15.7 kcal/mol (**TSA6**), giving π complex **IMA7**. In the gas phase, **IMA7** is 0.5 kcal/mol lower than **TSA6**, but it is 0.6 kcal/mol higher than **TSA6** after thermal and solvent corrections. The entropy driving force then dissociates **IMA7** into **IMA8** (LPd(H)(Br)) and **3k** (the product). The step from **IMA6** to **IMA8** + **3k** is endergonic by 5.0 kcal/mol but can be driven by the subsequent catalyst regeneration, which is thermodynamically favorable (Figure S2 in the Supporting Information). The trans isomer of **IMA8**, **IMA8'**, is 20.3 kcal/mol above **IMA8** because of the strong trans influence between the hydride and the PPh₃ ligand. Alternatively, the β -hydride elimination could proceed along the blue pathway in Figure 2, leading to **3k'**. However, because of the large steric effect between the 'Bu and phenyl groups, as reflected by the structures of **TSA6** and **TSA6'**, the formation of **3k'** is much less favorable than that of **3k** in terms of both kinetics and thermodynamics, explaining our observed anti stereoselectivity (Table 1 and Scheme 2).

Previously, it has been shown that the pathway involving the monophosphine is energetically more favorable than the pathway involving the bisphosphine in palladium-catalyzed C–C coupling reactions.^{19b} We also used the monophosphine palladium complex (PPh₃Pd) as the active catalyst in our mechanistic computations. To confirm the reasonability of using PPh₃Pd, as mentioned above, we further used (PPh₃)₂Pd as the active catalyst to calculate the pathways for the oxidative addition and cyclization steps (steps 1 and 2). The results (Figure S3 in the Supporting Information) show that the pathway with (PPh₃)₂Pd as the active catalyst is kinetically and thermodynamically less favorable than that with PPh₃Pd as the active catalyst. Therefore, the active catalyst in the present reaction should also be monophosphine palladium complex PPh₃Pd, verifying the rationality of using PPh₃ as the active catalyst to investigate the mechanism of the reaction shown in eq 4.

Figure 3 presents the energetic and geometric results for steps 2 and 3 in the reaction shown in eq 5. Unlike the reaction in eq 4, the substrate ene-yne-ketone **11** cannot directly coordinate to the oxidation product **IMB2**, because, as shown by its structure,

the palladium center in **IMB2** is encompassed, leaving no site available for **11** coordination. Previously, Buchwald and co-workers revealed that the triisopropylbiphenyl substituent of XPhos needs to rotate around P–C₂ bond to expose the palladium center for catalysis and reported that it was difficult to locate the rotation transition state.²⁰ We also were not able to find the transition state. Similar to the approach used in Buchwald's study, we scanned the potential energy surface (PES) using the dihedral angle ($\angle C_1C_2PPd$) as the scanning coordinate (Figure S8 in the Supporting Information). On the basis of the PES, we estimate the enthalpy barrier to be about 19.0 kcal/mol relative to **IMB2**, and therefore, the rotation to transform **IMB2** into **IMB2'** is feasible. Subsequently, **IMB2'** adjusts to give **IMB3** via **TSB2'**, resulting in a structure suitable for coordination of **11**. The pathway from **IMB3** to **IMB6** in Figure 3 is similar to that from **IMA3** to **IMA6** in Figure 1 except for the energetic differences. Again, a palladium carbene species (**IMB5**) is involved. Because of the trans influence of the phosphine ligand,²³ the Pd=C bond (1.986 Å) in **IMB5** is slightly longer than the one in **IMA5** (1.975 Å; Figure 1), and the Wiberg bond index (0.631) in **IMB5** is slightly less than that in **IMA5** (0.699). Nevertheless, the palladium species **IMB5** also has σ and π orbitals involved in the formal Pd=C double bond, similar to those in **IMA5** (Figure S7 in the Supporting Information). The palladium carbene **IMB5** then undergoes migratory insertion via a barrier of 3.6 kcal/mol, forming **IMB6**. Overall, the process from **IMB2** + **11** to **IMB6** overcomes a barrier of 26.1 kcal/mol and is exergonic by 32.8 kcal/mol.

The pathway for the β -hydride elimination in the reaction in eq 5 is shown in Figure 4. Unlike the corresponding step in the reaction in eq 4, which has two possible pathways (Figure 2), the β -hydride elimination from **IMB6** can lead to only one product, **5b**, because the hydride transfer takes place on the CH₃ group rather than CH₂Ph group in eq 4. To undergo β -hydride elimination, **IMB6** first needs to isomerize to **IMB7**, in which H ^{β} interacts with the Pd center via an agostic interaction. The isomerization breaks the π coordination between the phenyl group and the Pd center, resulting in an energy increase by 9.5 kcal/mol in going from **IMB6** to **IMB7**. Subsequently, the β -hydride elimination proceeds via **TSB7**, leading to π complex

IMB8, which is 7.2 kcal/mol lower than TSB7 in the gas phase but 1.7 kcal/mol higher than TSB7 after thermal and solvent corrections. Finally, the product **5b** is released from IMB8. The resulting species IMB9 can readily isomerize to a more stable complex, IMB10, which then enters the catalyst recovery step (Figure S6 in the Supporting Information). Similar to the β -hydride elimination in the reaction in eq 4, the step is endergonic by 3.5 kcal/mol and needs the thermodynamic driving force from the catalyst recovery step.

CONCLUSION

We have developed a palladium-catalyzed cross-coupling reaction between ene-yne-ketones and benzyl, aryl, or allyl bromides. These transformations represent a novel synthetic method to produce various 2-alkenyl-substituted furans in moderate to good yields. Moreover, computational studies support our hypothesis that palladium carbene formation and subsequent migratory insertion are the key steps in the catalytic cycle. The implication of this study is that palladium carbene migratory insertion can be considered as a general and facile process that occurs under suitable conditions regardless of the carbene precursors. This may open up new possibilities for developing novel transformations based on palladium carbene migratory insertions.

ASSOCIATED CONTENT

Supporting Information

Experimental procedures, characterization data, copies of ^1H and ^{13}C NMR spectra, and details and complete results of the DFT calculations. This material is available free of charge via the Internet at <http://pubs.acs.org>.

AUTHOR INFORMATION

Corresponding Authors

zxwang@ucas.ac.cn

wangjb@pku.edu.cn

Author Contributions

$^{\text{S}}$ Y.X., S.Q., and Q.X. contributed equally.

Notes

The authors declare no competing financial interest.

ACKNOWLEDGMENTS

This project was supported by the National Natural Science Foundation of China (Grant 21272010 and 21332002) and the National Basic Research Program of China (973 Program, 2012CB821600).

REFERENCES

- (1) For reviews, see: (a) Zhang, Y.; Wang, J. *Eur. J. Org. Chem.* **2011**, 1015–1026. (b) Barluenga, J.; Valdés, C. *Angew. Chem., Int. Ed.* **2011**, *50*, 7486–7500. (c) Shao, Z.; Zhang, H. *Chem. Soc. Rev.* **2012**, *41*, 560–572. (d) Xiao, Q.; Zhang, Y.; Wang, J. *Acc. Chem. Res.* **2013**, *46*, 236–247.
- (2) For most recent examples, see: Pd-catalyzed reactions: (a) Chen, Z.-S.; Duan, X.-H.; Zhou, P.-X.; Ali, S.; Luo, J.-Y.; Liang, Y.-M. *Angew. Chem., Int. Ed.* **2012**, *51*, 1370–1374. (b) Roche, M.; Hamze, A.; Provot, O.; Brion, J.-D.; Alami, M. *J. Org. Chem.* **2013**, *78*, 445–454. (c) Xia, Y.; Hu, F.; Liu, Z.; Qu, P.; Ge, R.; Ma, C.; Zhang, Y.; Wang, J. *Org. Lett.* **2013**, *15*, 1784–1787. Cu-catalyzed reactions: (d) Ye, F.; Ma, X.; Xiao, Q.; Li, H.; Zhang, Y.; Wang, J. *J. Am. Chem. Soc.* **2012**, *134*, 5742–5745. (e) Hu, M.; Ni, C.; Hu, J. *J. Am. Chem. Soc.* **2012**, *134*, 15257–15260. (f) Xiao, Q.; Ling, L.; Ye, F.; Tan, R.; Tian, L.; Zhang, Y.; Li, Y.; Wang, J. *J. Org. Chem.* **2013**, *78*, 3879–3885. Ni- and Co-catalyzed reactions:

- (g) Yao, T.; Hirano, K.; Satoh, T.; Miura, M. *Angew. Chem., Int. Ed.* **2012**, *51*, 775–779. Rh-catalyzed reactions: (h) Chan, W.-W.; Lo, S.-F.; Zhao, Z.; Yu, W.-Y. *J. Am. Chem. Soc.* **2012**, *134*, 13565–13568. (i) Selander, N.; Worrell, B. T.; Chuprakov, S.; Velaparthi, S.; Fokin, V. V. *J. Am. Chem. Soc.* **2012**, *134*, 14670–14673. (j) Hyster, T. K.; Ruhl, K. E.; Rovis, T. *J. Am. Chem. Soc.* **2013**, *135*, 5364–5367.

- (3) For selected examples, see: (a) Yu, W.-Y.; Tsoi, Y.-T.; Zhou, Z.; Chan, A. S. C. *Org. Lett.* **2009**, *11*, 469–472. (b) Xiao, Q.; Ma, J.; Yang, Y.; Zhang, Y.; Wang, J. *Org. Lett.* **2009**, *11*, 4732–4735. (c) Barluenga, J.; Moriel, P.; Valdés, C.; Aznar, F. *Angew. Chem., Int. Ed.* **2007**, *46*, 5587–5590. (d) Peng, C.; Yan, G.; Wang, Y.; Jiang, Y.; Zhang, Y.; Wang, J. *Synthesis* **2010**, 4154–4168. (e) Chen, S.; Wang, J. *Chem. Commun.* **2008**, 4198–4200. (f) Kudirka, R.; Devine, S. K. J.; Adams, C. S.; Van Vranken, D. L. *Angew. Chem., Int. Ed.* **2009**, *48*, 3677–3680. (g) Zhang, Z.; Liu, Y.; Gong, M.; Zhao, X.; Zhang, Y.; Wang, J. *Angew. Chem., Int. Ed.* **2010**, *49*, 1139–1142. (h) Chen, Z.-S.; Duan, X.-H.; Wu, L.-Y.; Ali, S.; Ji, K.-G.; Zhou, P.-X.; Liu, X.-Y.; Liang, Y.-M. *Chem.—Eur. J.* **2011**, *17*, 6918–6921. (i) Zhang, Z.; Liu, Y.; Ling, L.; Li, Y.; Dong, Y.; Gong, M.; Zhao, X.; Zhang, Y.; Wang, J. *J. Am. Chem. Soc.* **2011**, *133*, 4330–4341.
- (4) (a) Peng, C.; Wang, Y.; Wang, J. *J. Am. Chem. Soc.* **2008**, *130*, 1566–1567. (b) Tsoi, Y.-T.; Zhou, Z.; Chan, A. S. C.; Yu, W.-Y. *Org. Lett.* **2010**, *12*, 4506–4509. (c) Zhao, X.; Jing, J.; Lu, K.; Zhang, Y.; Wang, J. *Chem. Commun.* **2010**, 46, 1724–1726. (d) Zhou, L.; Ye, F.; Ma, J.; Zhang, Y.; Wang, J. *Angew. Chem., Int. Ed.* **2011**, *50*, 3510–3514.

- (5) Palladium carbenes have been suggested as reactive intermediates in catalytic reactions. For examples, see: (a) Trost, B. M.; Tanoury, G. J. *J. Am. Chem. Soc.* **1988**, *110*, 1636–1638. (b) Trost, B. M.; Hashmi, A. S. K. *Angew. Chem., Int. Ed. Engl.* **1993**, *32*, 1085–1087. (c) Schweizer, S.; Song, Z.-Z.; Meyer, F. E.; Parsons, P. J.; de Meijere, A. *Angew. Chem., Int. Ed.* **1999**, *38*, 1452–1454. (d) Nakamura, I.; Bajracharya, G. B.; Mizushima, Y.; Yamamoto, Y. *Angew. Chem., Int. Ed.* **2002**, *41*, 4328–4331. (e) Fillion, E.; Taylor, N. J. *J. Am. Chem. Soc.* **2003**, *125*, 12700–12701. (f) Shi, M.; Liu, L.-P.; Tang, J. *J. Am. Chem. Soc.* **2006**, *128*, 7430–7431. (g) Trépanier, V. É.; Fillion, E. *Organometallics* **2007**, *26*, 30–32.

- (6) For studies of stable palladium carbene species, see: (a) Albéniz, A. C.; Espinet, P.; Manrique, R.; Pérez-Mateo, A. *Angew. Chem., Int. Ed.* **2002**, *41*, 2363–2366. (b) Danopoulos, A. A.; Tsoureas, N.; Green, J. C.; Hursthouse, M. B. *Chem. Commun.* **2003**, 756–757. (c) Bröring, M.; Brandt, C. D.; Stellwag, S. *Chem. Commun.* **2003**, 2344–2345. (d) Solé, D.; Vallverdú, L.; Solans, X.; Font-Bardia, M.; Bonjoch, J. *Organometallics* **2004**, *23*, 1438–1447. (e) Albéniz, A. C.; Espinet, P.; Manrique, R.; Pérez-Mateo, A. *Chem.—Eur. J.* **2005**, *11*, 1565–1573. (f) Albéniz, A. C.; Espinet, P.; Pérez-Mateo, A.; Nova, A.; Ujaque, G. *Organometallics* **2006**, *25*, 1293–1297. (g) López-Alberca, M. P.; Manchego, M. J.; Fernández, I.; Gómez-Gallego, M.; Sierra, M. A.; Torres, R. *Org. Lett.* **2007**, *9*, 1757–1759. (h) Meana, I.; Albéniz, A. C.; Espinet, P. *Organometallics* **2012**, *31*, 5494–5499.

- (7) For selected reviews of diazo compounds, see: (a) Ye, T.; McKervey, M. A. *Chem. Rev.* **1994**, *94*, 1091–1160. (b) Doyle, M. P.; McKervey, M. A.; Ye, T. *Modern Catalytic Methods for Organic Synthesis with Diazo Compounds*; Wiley: New York, 1998. (c) Davies, H. M. L.; Beckwith, R. E. J. *Chem. Rev.* **2003**, *103*, 2861–2903. (d) Zhang, Z.; Wang, J. *Tetrahedron* **2008**, *64*, 6577–6605.

- (8) For selected reviews, see: (a) Miki, K.; Uemura, S.; Ohe, K. *Chem. Lett.* **2005**, *34*, 1068–1077. (b) Hashmi, A. S. K. *Chem. Rev.* **2007**, *107*, 3180–3211. (c) Fürstner, A.; Davies, P. W. *Angew. Chem., Int. Ed.* **2007**, *46*, 3410–3449. (d) Michelet, V.; Toullec, P. Y.; Genêt, J.-P. *Angew. Chem., Int. Ed.* **2008**, *47*, 4268–4315. (e) Jiménez-Núñez, E.; Echavarren, A. M. *Chem. Rev.* **2008**, *108*, 3326–3350. (f) Fürstner, A. *Chem. Soc. Rev.* **2009**, *38*, 3208–3221. For a related report on palladium-catalyzed cycloisomerization of terminal allenyl ketones for the synthesis of furans, see: (g) Hashmi, A. S. K.; Ruppert, T. L.; Knöfel, T.; Bats, J. W. *J. Org. Chem.* **1997**, *62*, 7295–7304.

- (9) (a) Ohe, K.; Yokoi, T.; Miki, K.; Nishino, F.; Uemura, S. *J. Am. Chem. Soc.* **2002**, *124*, 526–527. (b) Ohe, K.; Yokoi, T.; Miki, K.; Nishino, F.; Uemura, S. *J. Am. Chem. Soc.* **2002**, *124*, 5260–5261. (c) Kato, Y.; Miki, K.; Nishino, F.; Ohe, K.; Uemura, S. *Org. Lett.* **2003**, *5*, 2619–2621. (d) Miki, K.; Yokoi, T.; Nishino, F.; Kato, Y.; Washitake, Y.;

Ohe, K.; Uemura, S. *J. Org. Chem.* **2004**, *69*, 1557–1564. (e) Miki, K.; Washitake, Y.; Ohe, K.; Uemura, S. *Angew. Chem., Int. Ed.* **2004**, *43*, 1857–1860.

(10) (a) Vicente, R.; González, J.; Riesgo, L.; González, J.; López, L. A. *Angew. Chem., Int. Ed.* **2012**, *51*, 8063–8067. (b) González, J.; González, J.; Pérez-Calleja, C.; López, L.; Vicente, R. *Angew. Chem., Int. Ed.* **2013**, *52*, 5853–5857.

(11) (a) Wang, T.; Zhang, J. *Dalton Trans.* **2010**, *39*, 4270–4273. (b) Cao, H.; Zhan, H.; Cen, J.; Lin, J.; Lin, Y.; Zhu, Q.; Fu, M.; Jiang, H. *Org. Lett.* **2013**, *15*, 1080–1083. (c) Zhan, H.; Lin, X.; Qiu, Y.; Du, Z.; Li, P.; Li, Y.; Cao, H. *Eur. J. Org. Chem.* **2013**, 2284–2287.

(12) For other related reports, see: (a) Herndon, J. W.; Wang, H. *J. Org. Chem.* **1998**, *63*, 4564–4565. (b) Nishino, F.; Miki, K.; Kato, Y.; Ohe, K.; Uemura, S. *Org. Lett.* **2003**, *5*, 2615–2617. (c) Barluenga, J.; Riesgo, L.; Vicente, R.; López, L. A.; Tomás, M. *J. Am. Chem. Soc.* **2008**, *130*, 13528–13529. (d) Murata, T.; Murai, M.; Ikeda, Y.; Miki, K.; Ohe, K. *Org. Lett.* **2012**, *14*, 2296–2299. (e) Clark, J. S.; Boyer, A.; Aimon, A.; García, P. E.; Lindsay, D. M.; Symington, A. D. F.; Danoy, Y. *Angew. Chem., Int. Ed.* **2012**, *51*, 12128–12131.

(13) See the Supporting Information for details.

(14) For a detailed discussion of the effect of base on transition-metal-catalyzed coupling reactions, see: Ouyang, K.; Xi, Z. *Acta Chim. Sin.* **2013**, *71*, 13–25.

(15) Similar *E/Z* isomerization has been observed previously; see the supporting information for ref 12e.

(16) (a) Busacca, C. A.; Swestock, J.; Johnson, R. E.; Bailey, T. R.; Musza, L.; Rodger, C. A. *J. Org. Chem.* **1994**, *59*, 7553–7556. (b) Farina, V.; Hossain, M. A. *Tetrahedron Lett.* **1996**, *37*, 6997–7000. (c) Xiao, F.; Wang, J. *J. Org. Chem.* **2006**, *71*, 5789–5791. (d) Shi, W.; Xiao, F.; Wang, J. *J. Org. Chem.* **2005**, *70*, 4318–4322.

(17) Frisch, M. J.; Trucks, G. W.; Schlegel, H. B.; Scuseria, G. E.; Robb, M. A.; Cheeseman, J. R.; Scalmani, G.; Barone, V.; Mennucci, B.; Petersson, G. A.; Nakatsuji, H.; Caricato, M.; Li, X.; Hratchian, H. P.; Izmaylov, A. F.; Bloino, J.; Zheng, G.; Sonnenberg, J. L.; Hada, M.; Ehara, M.; Toyota, K.; Fukuda, R.; Hasegawa, J.; Ishida, M.; Nakajima, T.; Honda, Y.; Kitao, O.; Nakai, H.; Vreven, T.; Montgomery, J. A., Jr.; Peralta, J. E.; Ogliaro, F.; Bearpark, M.; Heyd, J. J.; Brothers, E.; Kudin, K. N.; Staroverov, V. N.; Kobayashi, R.; Normand, J.; Raghavachari, K.; Rendell, A.; Burant, J. C.; Iyengar, S. S.; Tomasi, J.; Cossi, M.; Rega, N.; Millam, N. J.; Klene, M.; Knox, J. E.; Cross, J. B.; Bakken, V.; Adamo, C.; Jaramillo, J.; Gomperts, R.; Stratmann, R. E.; Yazyev, O.; Austin, A. J.; Cammi, R.; Pomelli, C.; Ochterski, J. W.; Martin, R. L.; Morokuma, K.; Zakrzewski, V. G.; Voth, G. A.; Salvador, P.; Dannenberg, J. J.; Dapprich, S.; Daniels, A. D.; Farkas, Ö.; Foresman, J. B.; Ortiz, J. V.; Cioslowski, J.; Fox, D. J. *Gaussian 09*, revision A.01; Gaussian, Inc.: Wallingford, CT, 2009.

(18) All of the energies were computed at the M06/BSII//B3LYP/BSI level. Solvent effects were taken into account by the SMD solvent model using DMF and CH₃CN as the solvents for eqs 4 and 5, respectively. BSII denotes a basis set of SDD for Pd and 6-311++G(d,p) for nonmetal atoms, and BSI denotes a basis set of LANL2DZ for Pd and 6-31G(d) for nonmetal atoms. The gas-phase B3LYP/BSI harmonic frequencies were used for thermal corrections to the free energies at 298.15 K and 1 atm. More details are given in the Supporting Information.

(19) (a) Christmann, U.; Vilar, R. *Angew. Chem., Int. Ed.* **2005**, *44*, 366–374. (b) Ahlquist, M.; Fristrup, P.; Tanner, D.; Norrby, P. O. *Organometallics* **2006**, *25*, 2066–2073. (c) Braga, A. A. C.; Ujaque, G.; Maseras, F. *Organometallics* **2006**, *25*, 3647–3658. (d) Ahlquist, M.; Norrby, P. O. *Organometallics* **2007**, *26*, 550–553. (e) Lam, K. C.; Marder, T. B.; Lin, Z. Y. *Organometallics* **2007**, *26*, 758–760. (f) Surawatanawong, P.; Fan, Y.; Hall, M. B. *J. Organomet. Chem.* **2008**, *693*, 1552–1563.

(20) (a) Hicks, J. D.; Hyde, A. M.; Cuezva, A. M.; Buchwald, S. L. *J. Am. Chem. Soc.* **2009**, *131*, 16720–16734. (b) Barder, T. E.; Buchwald, S. L. *J. Am. Chem. Soc.* **2007**, *129*, 12003–12010. (c) Barder, T. E.; Biscoe, M. R.; Buchwald, S. L. *Organometallics* **2007**, *26*, 2183–2192.

(21) For reports on the structure of palladium carbenes, see: (a) Taubmann, C.; Öfele, K.; Herdtweck, E.; Herrmann, W. A. *Organometallics* **2009**, *28*, 4254–4257. (b) Taubmann, C.; Tosh, E.;

Öfele, K.; Herdtweck, E.; Herrmann, W. A. *J. Organomet. Chem.* **2008**, *693*, 2231–2236. (c) Herrmann, W. A.; Öfele, K.; Taubmann, C.; Herdtweck, E.; Hoffmann, S. D. *J. Organomet. Chem.* **2007**, *692*, 3846–3854. (d) Schneider, S. K.; Roembke, P.; Julius, G. R.; Raubenheimer, H. G.; Herrmann, W. A. *Adv. Synth. Catal.* **2006**, *348*, 1862–1873. (e) Schuster, O.; Raubenheimer, H. G. *Inorg. Chem.* **2006**, *45*, 7997–7999. (f) Oulié, P.; Nebra, N.; Saffon, N.; Maron, L.; Martin-Vaca, B.; Bourissou, D. *J. Am. Chem. Soc.* **2009**, *131*, 3493–3498. (g) Weng, W.; Chen, C.-H.; Foxman, B. M.; Ozerov, O. V. *Organometallics* **2007**, *26*, 3315–3320. (h) Stander-Grobler, E.; Schuster, O.; Heydenrych, G.; Cronje, S.; Tosh, E.; Albrecht, M.; Frenking, G.; Raubenheimer, H. G. *Organometallics* **2010**, *29*, 5821–5833. (i) Kessler, F.; Szesni, N.; Pöhako, K.; Weibert, B.; Fischer, H. *Organometallics* **2009**, *28*, 348–354. (j) Vignolle, J.; Gornitzka, H.; Donnadiou, B.; Bourissou, D.; Bertrand, G. *Angew. Chem., Int. Ed.* **2008**, *47*, 2271–2274.

(22) (a) Wiberg, K. B. *Tetrahedron* **1968**, *24*, 1083–1096. (b) Reed, A. E.; Curtiss, L. A.; Weinhold, F. *Chem. Rev.* **1988**, *88*, 899–926.

(23) Appleton, T. G.; Clark, H. C.; Manzer, L. E. *Coord. Chem. Rev.* **1973**, *10*, 335–422.